Eur. Phys. J. D **38**, 537–544 (2006)
DOI: 10.1140/epjd/e2006-00056-8

THE EUROPEAN PHYSICAL JOURNAL D

Phase switching and quantum interference in a 3-level Λ-shape bistable model

K.I. Osman[1,a] and S.S. Hassan[2,b]

[1] Department of Mathematics, Al-Azhar University, Faculty of Science (Women's Section), P.O. Box 11754, Nasr City, Cairo, Egypt
[2] University of Bahrain, College of Science, Math. Dept., P.O. Box 32038, Bahrain

Received 29 July 2005 / Received in final form 7 January 2006
Published online 14 March 2006 –

Abstract. The steady state bistable behaviour of a three-level Λ-shape is examined in the presence of a control field $(\Omega + \chi(t)\, e^{i\varphi})$: Ω is the strong Rabi component, $\chi(t)$ is the stochastic part with relative phase φ; with quantum interference between decay channels taken into account. One- and two-way phase switching effect for the transmitted field against the phase are predicted at fixed values for the incident input field. Also cooperative switching effect shows multistable/bistable behaviour. Quantum interference tends to diminish the dispersive effects responsible for multistable behaviour (in the input-output relation and the cooperative switching diagram) and asymmetry (in the phase switching diagram). Equivalence of the role of the stochastic part of the control field with that of the "classically" squeezed field is shown to occur *only* in the absence of quantum interference.

PACS. 42.65.Pc Optical bistability, multistability, and switching, including local field effects – 42.65.-k Nonlinear optics

1 Introduction

Quantum coherence and interference effects associated with a three-level atomic systems have played a crucial role in controlling many phenomena (such as: electromagnetic induced transparency (EIT), lasing without inversion (LWI), optical multistability (OM)) in non-linear quantum optics [1,2]. Interestingly, OM has been observed in an EIT three-level Λ-shape atomic system in ^{78}Rb vapor cell inside an optical ring cavity [3]. The advantage of using atomic vapor cell (rather than atomic beam) allows to observe OM to a high value of the atomic density (or cooperation parameter). Phase control of amplitude-fluctuation-induced optical bistability has been theoretically investigated for the three-level Λ-shape atomic system placed in a ring cavity [4], where the control field amplitude (associated with the transition between the upper level $|2\rangle$ and the lower level $|1\rangle$, Fig. 1) comprises two terms $(\Omega + \chi(t)e^{i\varphi})$: Ω is strong Rabi frequency, $\chi(t)$ is weak stochastic field amplitude and φ is the relative phase between the two field components-which have the same frequency ω_1. A main conclusion in [4] is that the bandwidth of the stochastic field dephases the atomic coherence between level $|1\rangle$, $|3\rangle$ and hence the bistable behaviour may occur (also see [5]). Here, we extend the work of [4] by including the quantum interference (QI) effects and different detuning as well as exploring the multiple phase switching effect, by varying the relative phase φ for fixed values of the incident coherent field.

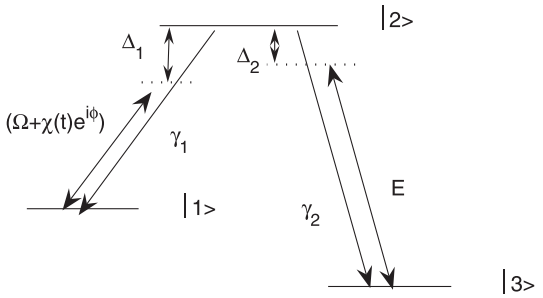

Fig. 1. The 3-level Λ-type scheme: the control field $(\Omega + \chi(t)e^{i\varphi})$ of frequency ω_1 couples the transition from level $|1\rangle \leftrightarrow |2\rangle$ while the cavity field E of frequency ω_c couples the transition $|3\rangle \leftrightarrow |2\rangle$. The decay rates γ_1, γ_2 from level $|2\rangle$ to level $|1\rangle$, $|3\rangle$ respectively.

2 The model master equation and state equation

The three-level atomic Λ-shape scheme is depicted in Figure 1. The three levels $|1\rangle$, $|2\rangle$, $|3\rangle$ have energies E_1, E_2, E_3 respectively. Atomic operators are represented as $A_{kj} = |k\rangle\langle j|$, $A_{kk} = |k\rangle\langle k|$. The control field $(\Omega + \chi(t)e^{i\varphi})$ couples levels $|2\rangle$, $|1\rangle$ while the other transition $|2\rangle \leftrightarrow |3\rangle$

[a] e-mail: kie_osman@hotmail.com
[b] e-mail: shoukryhassan@hotmail.com

is driven by the intracavity field of Rabi frequency E and oscillatory frequency ω_c.

The usual master equation approach (e.g. [6]) gives the equation for the reduced atomic density operator ρ_s within the rotating wave approximation ($\hbar = 1$ is taken throughout this paper) in the form,

$$\dot{\rho_s} = -i\left[H_1 + H_2, \rho_s\right] - i\left[H_3, \rho_s\right] + L\rho_s \tag{1}$$

where,

$$H_1 = \left(\Delta_2 - \Delta_1\right) A_{11} + \Delta_2 A_{22} - \frac{1}{2}\Omega\left(A_{12} + A_{21}\right), \tag{2}$$

$$H_2 = -\frac{1}{2}\chi\left(t\right)\left(e^{-i\varphi}A_{12} + e^{i\varphi}A_{21}\right), \tag{3}$$

$$H_3 = -\frac{1}{2}\left(EA_{23} + E^{*}A_{32}\right) \tag{4}$$

and

$$\begin{aligned} L\rho_s = {} & \gamma_1\left(2A_{12}\rho_s A_{21} - A_{22}\rho_s - \rho_s A_{22}\right) \\ & + \gamma_2\left(2A_{32}\rho_s A_{23} - A_{22}\rho_s - \rho_s A_{22}\right) \\ & + 2\gamma_{13}\left(A_{32}\rho_s A_{21} + A_{12}\rho_s A_{23}\right). \end{aligned} \tag{5}$$

The notations are: the detuning parameters $\Delta_1 = E_2 - E_1 - \omega_1$, $\Delta_2 = E_2 - E_3 - \omega_c$, γ_j is the spontaneous-decay constant of the exited level $|2\rangle$ to the sublevel $|j\rangle (j = 1, 3)$ and γ_{13} represents the effect of the quantum interference resulting from the cross coupling between the transitions $|2\rangle \leftrightarrow |1\rangle$ and $|2\rangle \leftrightarrow |3\rangle$, which is given by $\gamma_{13} = \sqrt{\gamma_1\gamma_2}p$ with the alignment parameter, $p = \mathbf{d}_{21}\cdot\mathbf{d}_{23}/(|\mathbf{d}_{21}||\mathbf{d}_{23}|)$ ($\mathbf{d}_{ij}$ = atomic dipole moment between levels $|i\rangle, |j\rangle$). If $p = 1$, then $\gamma_{13} = \sqrt{\gamma_1\gamma_2}$ and the interference effect is maximum when $\mathbf{d}_{21}$ is parallel to $\mathbf{d}_{23}$ while, if $\mathbf{d}_{21}$ is orthogonal to $\mathbf{d}_{23}$, then $p = 0$, $\gamma_{13} = 0$, and the quantum interference disappears. It should be noted that quantum interference processes (called by other authors "spontaneous generation of coherence", as well "vacuum induced coherence") in a 3-level Λ-type system may lead to symmetric coherent superposition of the two-lower states [7]. The existence of such coherence effect depends on the nonorthogonality of the concerned two dipole moments. This can be achieved, for example, by: (i) mixing of levels arising from internal fields, as observed in molecular sodium dimer where the excited sub-levels are superpositions of singlet and triplet states that are mixed by spin-orbit interaction [8], (ii) mixing of levels arising from external fields, by pre-selecting the polarization of the cavity field [9].

Now, the weak stochastic field component $\chi(t)$ is assumed to be a real Gaussian-Markovian random process, $\langle\chi(t)\rangle = 0$, and has the correlation function,

$$\langle\chi(t)\chi(t')\rangle = Dke^{-k|t-t'|} \tag{6}$$

with D, k are the strength and bandwidth parameters respectively. For $\Omega \gg \sqrt{Dk}$, $k \gg \gamma_1, \gamma_2$ the stochastic variable $\chi\left(t\right)$ can be adiabatically eliminated [10] from equation (1) giving rise to a time-averaged master equation for the reduced density operator (see Appendix A for outline),

$$\begin{aligned} \dot{\rho} = {} & -i\left[H_1 + H_3, \rho\right] + L\rho \\ & - \gamma_c\left\{\left[\left(A_{21} + e^{-2i\varphi}A_{12}\right), \left[B, \rho\right]\right]\right. \\ & \left. + \left[\left(A_{12} + e^{2i\varphi}A_{21}\right), \left[B^{+}, \rho\right]\right]\right\} \end{aligned} \tag{7}$$

where $\gamma_c = Dk/4$ and

$$\begin{aligned} B = {} & \int_0^\infty e^{-k\tau}\left(e^{iH_1\tau}A_{12}e^{-iH_1\tau}\right)d\tau \\ = {} & b_1A_{11} + b_2A_{22} + b_3A_{12} + b_4A_{21} = B^{+} \end{aligned} \tag{8}$$

with,

$$b_1 = -b_2 = \frac{\Omega\left(\Delta - ik\right)}{2k\left(k^2 + \Omega'^2\right)} \tag{9}$$

$$b_3 = \frac{\Omega^2}{2k\Omega'^2} + \frac{\left[k\Delta^2 + \Omega'^2\left(k + 2i\Delta\right)\right]}{2\Omega'^2\left(k^2 + \Omega'^2\right)} \tag{10}$$

$$b_4 = \frac{\Omega^2}{2k\left(k^2 + \Omega'^2\right)} \tag{11}$$

and $\Omega' = \sqrt{\Delta^2 + \Omega^2}$ is a generalized Rabi frequency and have assumed for simplicity that $\Delta_2 = \Delta_1/2 = \Delta$.

The equations for the density matrix elements according to equation (7) are:

$$\begin{aligned} \dot{\rho}_{11} = {} & -2\,\mathrm{Re}\left(\mu_1\right)\rho_{11} + 2\left[\gamma_1 + \mathrm{Re}\left(\mu_1\right)\right]\rho_{22} \\ & - \left(\frac{1}{2}i\Omega - 2\mu_2\right)\rho_{12} + \left(\frac{1}{2}i\Omega + 2\mu_2^{*}\right)\rho_{21} \end{aligned} \tag{12}$$

$$\dot{\rho}_{33} = 2\gamma_2\rho_{22} + \frac{1}{2}iE^{*}\rho_{23} - \frac{1}{2}iE\rho_{32} \tag{13}$$

$$\begin{aligned} \dot{\rho}_{12} = {} & -\frac{1}{2}i\Omega\left(\rho_{11} - \rho_{22}\right) - \left(\gamma_1 + \gamma_2 - i\Delta + 2\mu_1^{*}\right)\rho_{12} \\ & + 2\mu_1 e^{-2i\varphi}\rho_{21} - \frac{1}{2}iE^{*}\rho_{13} \end{aligned} \tag{14}$$

$$\begin{aligned} \dot{\rho}_{13} = {} & 2\gamma_{13}\rho_{22} + \left(\frac{1}{2}i\Delta - \mu_1^{*}\right)\rho_{13} \\ & + \left(\frac{1}{2}i\Omega + \mu_2^{*}\right)\rho_{23} - \frac{1}{2}iE\rho_{12} \end{aligned} \tag{15}$$

$$\begin{aligned} \dot{\rho}_{23} = {} & -\left(\gamma_1 + \gamma_2 + \frac{1}{2}i\Delta + \mu_1\right)\rho_{23} + \left(\frac{1}{2}i\Omega - \mu_2\right)\rho_{13} \\ & + \frac{1}{2}iE\left(\rho_{33} - \rho_{22}\right) \end{aligned} \tag{16}$$

with the trace condition $\sum_i \rho_{ii} = 1$ and $\mu_1 = \gamma_c(b_3 + b_4^{*}e^{2i\varphi})$, $\mu_2 = \gamma_c(b_1 + b_1^{*}e^{2i\varphi})$.

Note that in the above equations, the QI manifests itself *only* in the spontaneous decay of level $|2\rangle$ that contributes to the coherence ρ_{13} (the term $2\gamma_{13}\rho_{22}$) in equation (15).

In the absence of QI (i.e.; $\gamma_{13} = 0$), the above equations are different from those in reference [4], resulting to different assumption of the detuning as mentioned before.

Now, consider a single mode ring cavity of length L (Fig. 2) containing an atomic medium of N homogeneously

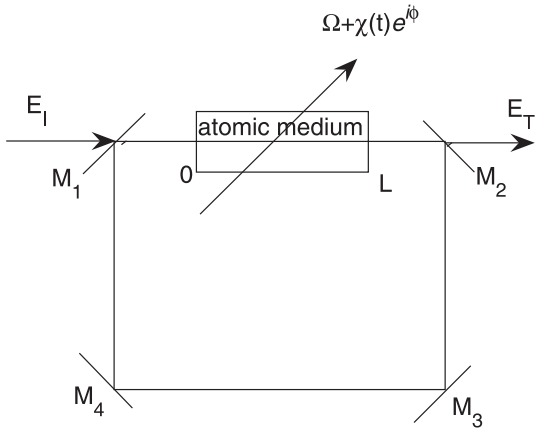

Fig. 2. The ring cavity configuration with plane mirrors M_i $(i = 1\text{–}4)$.

broadened three-level atoms of Λ-shape as in Figure 1; with an input field E_I at the mirror M_1 propagates in the z-directions, and the transmitted field is E_T at the mirror M_2. The two mirrors M_1, M_2 have reflectivity R and transmitivity T, while mirrors M_3 and M_4 have 100% reflectivity. The boundary conditions for the perfect tuned cavity field amplitude $E(z,t)$ at $z = 0, L$ in the steady-state limit are in the form [11]

$$E(0) = \sqrt{T}E_I + RE(L) \tag{17}$$

$$E_T = \sqrt{T}E(L). \tag{18}$$

In the mean-field limit, using the boundary conditions equations (17), (18) and the slowly varying Maxwell's equation

$$\frac{\partial E}{\partial t} + c\frac{\partial E}{\partial z} = 2\pi i d_{32}^2 \omega_c N \rho_{23} \tag{19}$$

the input-output (steady-state) relationship is

$$y = x - 2iC\rho_{23} \tag{20}$$

where $y = E_I/\gamma_2\sqrt{T}$ and $x = E_T/\gamma_2\sqrt{T}$ are the input and output field amplitudes, scaled in unit γ_2 respectively, and $C = \pi N \omega_c d_{32}^2 L/cT$ is the cooperative parameter.

In the following section we examine numerically the steady state input-output relation, equation (20) with equations (12–16), as well the 'phase' and 'cooperative' switching effects in the absence $(p = 0)$ and presence $(p \neq 0)$ of the QI terms.

3 Numerical results

We measure all quantities in equations (12–16) in terms of γ_2, we take the data: $\Omega/\gamma_2 = 30$, $k/\gamma_2 = 20$, $D/\gamma_2 = 0.2$, $\gamma_1/\gamma_2 = 1$ and $C = 4 \times 10^4$.

3.1 Phase switching with no quantum interference ($\mathbf{p = 0}$)

At exact resonance $(\Delta = 0)$ the 3-D plot $(|y|, |x|, \varphi)$ together with the 2-D plot of $|x|$ versus $|y|$ for different values of the phase φ are presented in Figures 3a and 3b. For $\varphi = \pi/2$ there is no bistable behaviour, while for $\varphi = 0, \pi/4$ bistable behaviour occurs with lower threshold value at $\varphi = 0$. Switching diagram showing the variation of the output field $|x|$ against the phase φ at fixed incident field values $|y| = 156.5$ and 178 are given in Figures 3c and 3d. Figure 3c shows one-way switching (switch-off): at $\varphi = 0$ if the system is on the upper branch (full line in Fig. 3b) and as φ increases the point (k_1) moves on the steady state curve until it reaches the unstable point (k) in Figure 3c and jumps down to the lower stable branch and keeps varying with increasing φ — but — with no further jumps. In Figure 3d at $\varphi = \pi/4$ if the system is at the point k_2' (Fig. 3b), and by increasing or decreasing φ, the system switches-on to the stable upper branch with no further jumps as φ changes.

In the off-resonance case $(\Delta/\gamma_2 = 0.1)$ the bistable behaviour now occurs for $\varphi = \pi/2$ and longer hysteresis cycle shows for $\varphi = 0$. Possible multistable behaviour may also occur for $\varphi = \pi/4$ (and $3\pi/8$)- an indication of higher nonlinearity due to interplay between dispersive effects and phase-dependent terms $(i\Delta/2 + \mu_1)$ in equations (14–16) for the coherences ρ_{ij} $(i \neq j)$.

The switching diagram is shown for fixed $|y| = 95$ and 96 in Figures 4a and 4b respectively. At $\varphi = 3\pi/8$, if the system is at the point (s_2) on the upper branch — see inset $|x| - |y|$ curve in Figure 4b — and as φ changes two possible switching-down processes can occur to the lower stable branch. The slight change in the fixed value of $|y|$ to 96 (Fig. 4c) merges the isolated isle in Figure 4b with the lower branch, and a two-way switching behaviour is exhibited $(a \to a',\ b \to b')$. Note that in this dispersive case $(\Delta \neq 0)$ the switching diagram is asymmetrical with respect to φ at $(\pi/2)$ unlike the resonant case in Figures 3c and 3d.

3.2 Phase switching with quantum interference ($\mathbf{p \neq 0}$)

Another significant effect on the optical bistability is the quantum interference with the variation of the relative phase. We display this effect in Figure 5 for the case of perfect interference $(p = 1)$. The threshold value for the bistable curve for any value of φ, increases considerably as shown in the 3-D plot of Figure 5a at exact resonance $(\Delta = 0)$, and the hysteresis cycle narrows with increasing the relative phase from 0 to $\pi/2$ then gradually enlarged when φ increases from $\pi/2$ to π. These results might be useful to control the threshold value and the hysteresis cycle width of the bistability curve when the parameter p takes optimal values. The switching diagram in this case is shown in Figures 5b and 5c for fixed values of $|y| = 178$ and 213.2. This is similar to the switching-down diagram of Figure 4b *but* symmetrically with respect to $\varphi = \pi/2$. Hence quantum interference for suitable values of the fixed input field $|y|$ diminishes the dispersive effect [12] and phase switching effect becomes symmetric as in the absorptive case of Figure 3. Therefore, effects of quantum interference in the spontaneous emission and the relative control phase are very useful in optimizing and controlling

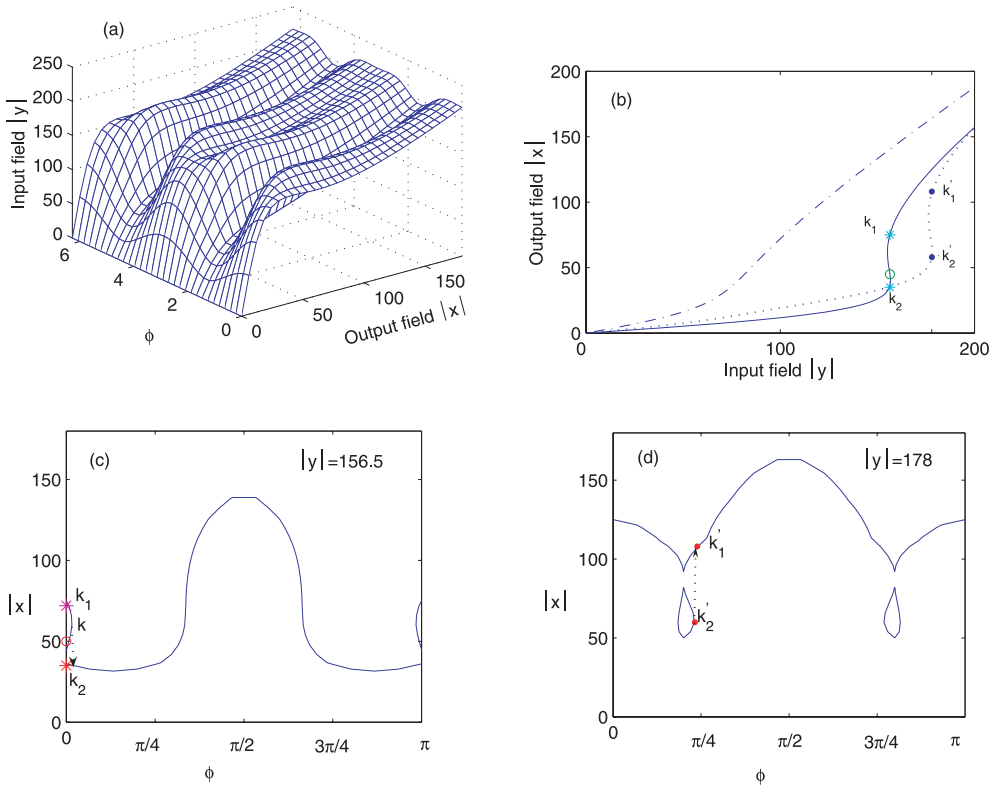

Fig. 3. (a) The 3-D plot for the incident field $|y|$ versus the transmitted field $|x|$ and the relative phase φ of the control field, for $C = 4 \times 10^4$, $\Omega/\gamma_2 = 30$, $k/\gamma_2 = 20$, $D/\gamma_2 = 0.2$, $\gamma_1/\gamma_2 = 1$, $\Delta = 0$, $p = 0$. (b) The variation of $|x|$ with $|y|$ for same data as (a) and different values of the relative phase φ: $\varphi = 0$ (solid line), $\varphi = \pi/4$ (dotted line) and $\varphi = \pi/2$ (dash-dot line). (c), (d) The phase switching diagram ($|x|$ against φ) at fixed $|y| = 156.5, 178$ respectively.

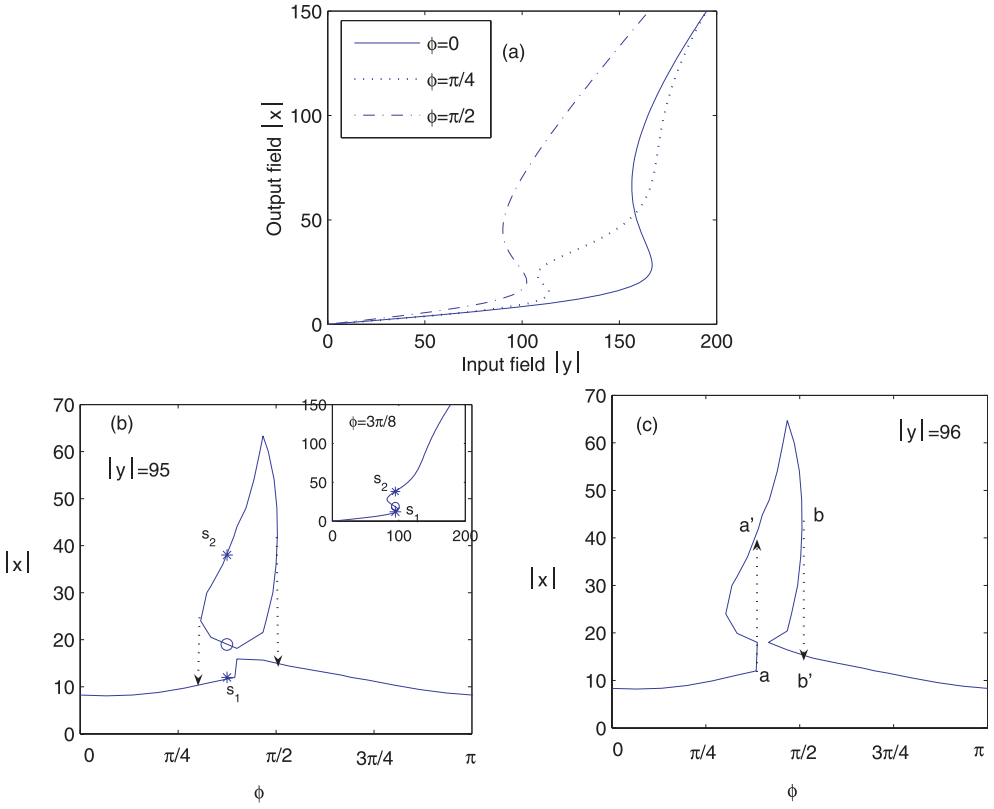

Fig. 4. (a) As Figure 3b but for $\Delta/\gamma_2 = 0.1$. (b), (c) As Figures 3c and 3d but for $\Delta/\gamma_2 = 0.1$ at $|y| = 95, 96$ respectively.

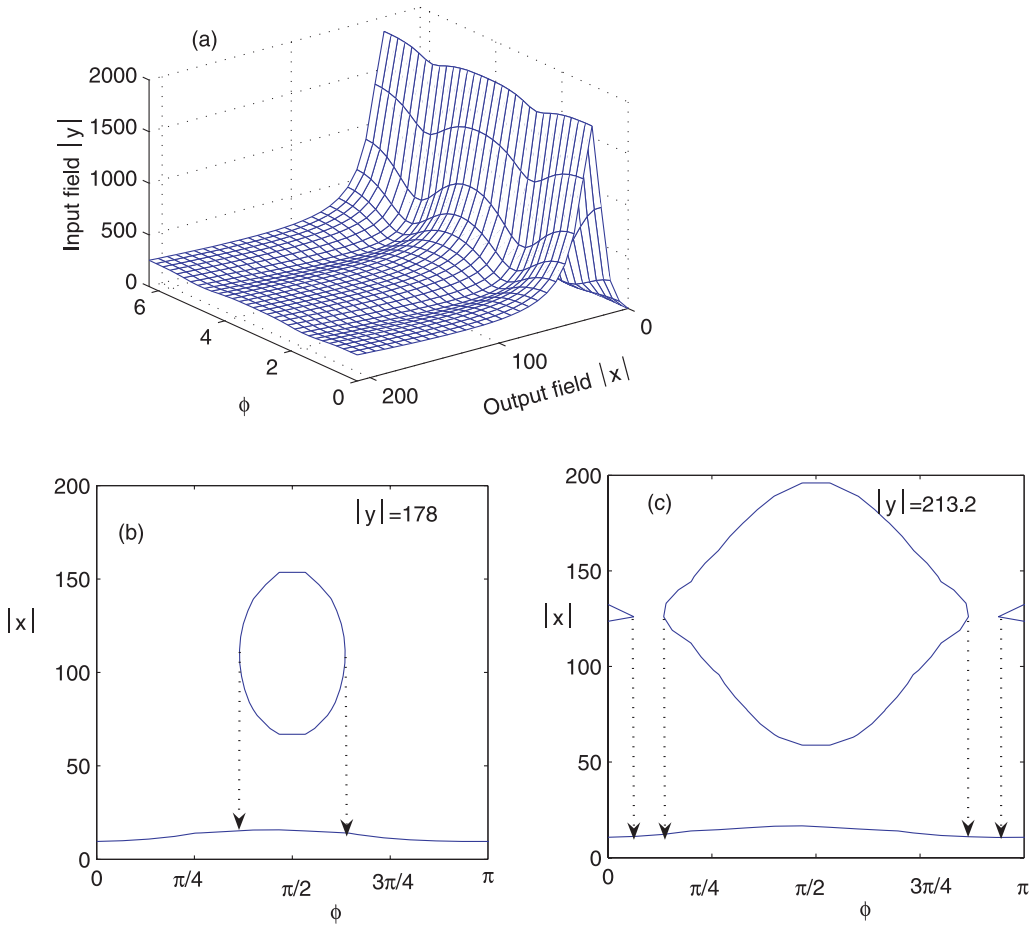

Fig. 5. (a) As Figure 3a but for $p = 1$. (b), (c) As Figures 3c and 3d but for $p = 1$ and $|y| = 178$, 213.2 respectively.

the optical switching process with dominant effect of the stochastic field.

3.3 Cooperative switching

In Figures 6a and 6b, we present the switching behaviour of the output field $|x|$ as the cooperative parameter C vary with fixed value of input field $|y| = 300$ at resonance ($\Delta = 0$) and off-resonance ($\Delta = 0.1$) for different values of the relative phase φ in the absence of quantum interference ($p = 0$). For certain values of the phase $\varphi = 3\pi/8$, $\pi/4$, the "nearly" transistor action in the absorptive regime (Fig. 6a) is changed to multistable behaviour due to dispersive effect (Fig. 6b) (similar behaviour occurs in the mesoscopic multi-stable regime [13]). The effect of quantum interference ($p = 1$) makes the switching-on value occurs at very small values of C (i.e. low atomic density) as well *independent* of the phase value φ in both absorptive and dispersive cases as shown in Figures 6c and 6d.

4 Summary

We have investigated the bistable model of three-level Λ-shape atomic structure placed in a ring cavity with control field $(\Omega + \chi(t)e^{i\varphi})$ couples the transition between the upper level and one of the two lower levels. Our investigation extends those of [4] by including the quantum interference (QI) effect due to the two decay channels, different detuning and also by exploring the phase as well as cooperative switching behaviour of the transmitted field against the relative phase φ of the control field and against the cooperation parameter. Our main results are:

(1) in the absence of QI multistable behaviour in the input-output relation occurs due to dispersive effects combined with certain values of the relative control phase parameter φ. Also, one-or two-way "phase switching" effect occurs in the relation between the output field and the relative control phase for certain values of the system parameters. These phase switching effects are similar to that found for 2-level bistable model in contact with squeezed vacuum reservoir [14,15]. The effect of QI is: (i) to increase the threshold value of $|y|$ in the bistable curve for any value of φ, (ii) to diminish the dispersive effect responsible for multi-stable behaviour, and (iii) to delete asymmetry in the phase switching diagram caused by the dispersive effect;
(2) in the "cooperative switching" diagram (relation between the output field and the cooperative parameter

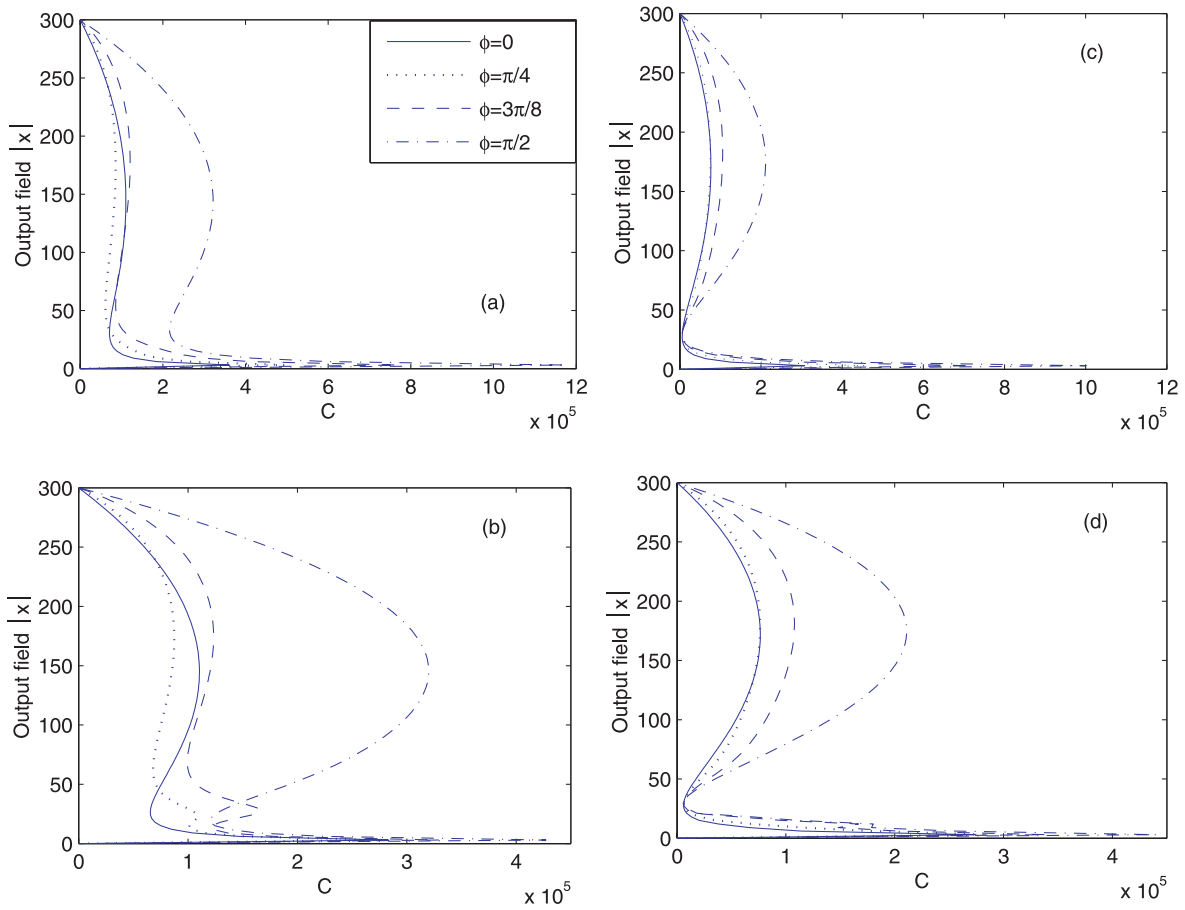

Fig. 6. (a) The cooperative switching diagram ($|x|$ against the cooperative parameter C) for $|y| = 300$, $p = 0$, $\Delta = 0$ and various values of φ. (b) As (a) but for $\Delta/\gamma_2 = 0.1$. (c), (d) As (a) and (b) respectively but for $p = 1$.

C) and in the absence of QI, "transistor action" found in the absorptive case which turned to multistable behaviour in the dispersive case. These, transistor action, bi- or multi-stable behaviour in the $(C - |x|)$ diagram resembles those found for mesoscopic multistable systems (amplifier regime [16], initially prepared atomic coherent state regime [13], 2-photon 2-level atom regime [17]) and also for dissipative 2-level bistable model with squeezed vacuum field input [18]. The effect of QI is: (i) to lower the threshold value of C, which becomes independent of the relative control phase φ, and (ii) to eliminate both the transistor action and multistable behaviour as mentioned above;

(3) as shown in the appendix when the stochastic part of the control field is replaced by "classical" squeezed vacuum field [19] interacting with the same levels $|1\rangle$, $|2\rangle$ the resulting density matrix equations are the same as equations (12–16) *only* in the absence of the QI.

Appendix

(1) First, we outline the standard perturbation techniques (cf. [10]) to eliminate the weak stochastic variable $\chi(t)$, from the density matrix equations (1–5), with correlations function given by (6) and for $\Omega \gg \sqrt{Dk}$, $k > \gamma_{1,2}$. First we temporarily disregard the last two terms of equation (1); since these quantity undergoes no change in the elimination procedure; then make the canonical transformation,

$$\tilde{\rho}_s = e^{iH_1 t}\rho_s e^{-iH_1 t} \tag{A.1}$$

which obeys the master equation

$$\dot{\tilde{\rho}}_s = -i\left[\tilde{H}_2(t), \tilde{\rho}_s\right] \tag{A.2}$$

where,

$$\tilde{H}_2(t) = -\frac{1}{2}\chi(t)F(t) \tag{A.3}$$

with

$$F(t) = e^{-i\varphi}A_{12}(t) + e^{i\varphi}A_{21}(t) \tag{A.4}$$

and

$$A_{12}(t) = A_{21}^{\dagger}(t) = e^{iH_1 t}A_{12}e^{-iH_1 t}. \tag{A.5}$$

Solving equation (A.2) with the help of the time dependent perturbation theory up to the second order in k yields

$$\dot{\tilde{\rho}}_s = -\int_0^t \left[\tilde{H}_2(t), \left[\tilde{H}_2(t'), \tilde{\rho}_s\right]\right] dt'. \tag{A.6}$$

Calculating the trace over the stochastic field ($\tilde{\rho} = \mathrm{Tr}_{stoch}\tilde{\rho}_s$) in equation (A.6) with the help of equation (6), making the change $t-t' = \tau$ and invoking the Markov approximation $\tilde{\rho}(t-\tau) \simeq \tilde{\rho}(t)$, the resulting master equation for the reduced density operator $\tilde{\rho}$ takes the form

$$\dot{\tilde{\rho}}(t) = -\frac{1}{4}Dk\int_0^\infty e^{-k\tau} \times \left(e^{-2i\varphi}\left[A_{12}(t), \left[A_{12}(t-\tau), \tilde{\rho}(t)\right]\right] + h.c.\right) d\tau - \frac{1}{4}Dk\int_0^\infty e^{-k\tau}\left(\left[A_{21}(t), \left[A_{12}(t-\tau), \tilde{\rho}(t)\right]\right] + h.c.\right) d\tau. \tag{A.7}$$

Transforming equation (A.7) to the original picture via

$$\rho = e^{iH_1 t}\tilde{\rho}e^{-iH_1 t} \tag{A.8}$$

and utilizing the Heisenberg-equations for H_1 and H_3 and restoring the $L\rho_s$ contribution, we obtain equation (7).

(2) Now, it worth noting that if the stochastic field $\chi(t)$ between levels $|1\rangle$, $|2\rangle$ is replaced by a broadband squeezed vacuum, the equations for the density matrix elements, in this case are [20]

$$\dot{\rho}_{11} = -2n_1\gamma_1\rho_{11} + 2\gamma_1(n_1+1)\rho_{22} - \frac{1}{2}i\Omega(\rho_{12}-\rho_{21}) - n_1\gamma_{13}(\rho_{13}+\rho_{31}) \tag{A.9}$$

$$\dot{\rho}_{33} = 2\gamma_2\rho_{22} + \frac{1}{2}iE^*\rho_{23} - \frac{1}{2}iE\rho_{32} - n_1\gamma_{13}(\rho_{13}+\rho_{31}) \tag{A.10}$$

$$\dot{\rho}_{12} = -\frac{1}{2}i\Omega(\rho_{11}-\rho_{22}) - [(2n_1+1)\gamma_1 + \gamma_2 - i\Delta]\rho_{12} + 2\gamma_1 m_1^*\rho_{21} - \frac{1}{2}iE^*\rho_{13} - 2m_1^*\gamma_{13}\rho_{23} - n_1\gamma_{13}\rho_{32} \tag{A.11}$$

$$\dot{\rho}_{13} = 2(n_1+1)\gamma_{13}\rho_{22} + \left(\frac{1}{2}i\Delta - n_1\gamma_1\right)\rho_{13} + \frac{1}{2}i\Omega\rho_{23} - \frac{1}{2}iE\rho_{12} - n_1\gamma_{13}\rho_{11} - n_1\gamma_{13}\rho_{33} \tag{A.12}$$

$$\dot{\rho}_{23} = -\left[(n_1+1)\gamma_1 + \gamma_2 + \frac{1}{2}i\Delta\right]\rho_{23} + \frac{1}{2}i\Omega\rho_{13} + \frac{1}{2}iE(\rho_{33}-\rho_{22}) - n_1\gamma_{13}\rho_{21} - 2m_1\gamma_{13}\rho_{12} \tag{A.13}$$

where n_1 and $|m_1|e^{i\Phi}$ are the squeezing parameters such that $|m_1|^2 \leq n_1(n_1+1)$ and Φ is the relative phase of the squeezed vacuum with respect to that of the coherent field.

In above equations (A.9–A.13) we notice that, the QI contributes spontaneously to the coherence ρ_{13} (just as in the case of stochastic part of the control field Eq. (15)), and in addition, is associated with the following stimulated processes:

(i) stimulated process associated with the occupations $\rho_{11}, \rho_{22}, \rho_{33}$ that contribute to the coherence ρ_{13} in equation (A.12);
(ii) the dispersive coherence ($2\,\mathrm{Re}(\rho_{13})$) that affects the occupation of the lower levels, ρ_{11}, ρ_{33} in equations (A.9) and (A.10);
(iii) the coherence ρ_{23} that affects the coherence ρ_{12} (and vice-versa) depending on the degree of the squeezing parameter m equations (A.11) and (A.13). Further, stimulated process associated with the coherence ρ_{32} contributes to the coherence ρ_{12} (and vice-versa).

The extra terms in equations (A.9–A.13) due to QI asserts the quantum nature of both QI and stimulated processes due to squeezed vacuum field.

The comparison of equations (A.9–A.13) with equations (12–16), in the absence of the quantum interference ($p = 0$), at exact resonance ($\Delta = 0$) for $\Phi = 2\varphi = 2n\pi (n = 0, 1, 2, ...)$, gives

$$n_1 = m_1 = \frac{D}{4\gamma_1} \tag{A.14}$$

where D is the strength parameter of the weak stochastic field.

This shows that the analogy between the case of weak stochastic field and that of squeezed vacuum with "classical analogue" ($n_1 = m_1$) (cf. [21]) is destroyed in presence of quantum interference.

References

1. M.O. Scully, M.S. Zubairy, *Quantum Optics* (Cambridge Univ. Press, Cambridge, 1997)
2. S. Alam, *Lasers without inversion and electromagnetically induced transparency* (SPIE Optical Engineering press, Bellingham, USA, 1999), see also work by T. Hänsch, R. Keil, A. Schabert, Ch. Schmelzer, P. Toschek, Z. Phys. **226**, 293 (1969); T. Hänsch, P. Toschek, Z. Phys. **236**, 213 (1970)
3. A. Joshi, M. Xiao, Phys. Rev. Lett. **91**, 143904 (2003); A. Joshi, A. Brown, H. Wang, M. Xiao, Phys. Rev. A **67**, 041801(R) (2003)
4. Xiang-Ming. Hu, Zhi-Zhan Xu, J. Opt. B: Quant. Semiclass. Opt. **3**, 35 (2001)
5. W. Harshawardhan, G.S. Agarwal, Phys. Rev. A **53**, 1812 (1996)
6. W.H. Louisell, *Quantum Statistical Properties of Radiation* (John Wiley & Sons, 1973)
7. J. Javanainen, Europhys. Lett. **17**, 407 (1991)
8. Hui-Rong Xia, Cen-Yun Ye, Shi-Yao Zhu, Phys. Rev. Lett. **77**, 1032 (1996)
9. K. Hakuta, L. Marmet, B.P. Stoicheff, Phys. Rev. Lett. **66**, 596 (1991); K. Hakuta, L. Marmet, B.P. Stoicheff, Phys. Rev. A **54**, 5152 (1992); S. Menon, G.S. Agarwal, Phys. Rev. A **57**, 4014 (1998); P.R. Berman, Phys. Rev. A **58**, 4886 (1998); A.K. Patnaik, G.S. Agarwal, Phys. Rev. A **59**, 3015 (1999); P. Zhou, S. Swain, Opt. Comm. **179**, 267 (2000)

10. N.G. Van Kampen, *Stochastic Processes in Physics and Chemistry* (North-Holland, Amsterdam, 1985); C.W. Gardiner, *Handbook of Stochastic Methods*, 2nd edn. (Springer-Verlag, 1985)
11. R. Bonifacio, L.A. Lugiato, Opt. Comm. **19**, 172 (1976); R. Bonifacio, L.A. Lugiato, Phys. Rev. A **18**, 1129 (1978)
12. S.S. Hassan, M.A. El-Deberky, Nonlin. Opt. Quant. Opt. **33**, 161 (2005)
13. S.S. Hassan, Y.A. Sharaby, J. Opt. B: Quant. Semiclass. Opt. **7**, S682 (2005)
14. P. Galatola, L.A. Lugiato, M. Porŕeca, P. Tombesi, Opt. Comm. **81**, 175 (1991)
15. S.S. Hassan, H.A. Batarfi, R. Saunders, R.K. Bullough, Eur. Phys. J. D **8**, 403 (2000)
16. M. Benassi, F. Casagrande, W. Lange, Quant. Semiclass. Opt. **9**, 879 (1997)
17. Y.A. Sharaby, S.S. Hassan, S.M.A. Maize, Nonlin. Opt. Quant. Opt. **33**, 1 (2005)
18. M.F.M. Ali, S.S. Hassan, S.M.A. Maize, J. Opt. B: Quant. Semiclass. Opt. **4**, 388 (2002)
19. Z. Ficek, P.D. Drummond, Phys. Today **50**, 34 (1997)
20. B.J. Dalton, Z. Ficek, S. Swain, J. Mod. Opt. **46**, 379 (1999)
21. P. Zhou, S. Swain, Phys. Rev. Lett. **82**, 2500 (1999)